Application of a generalized methodology for quantitative thermal diffusivity depth profile reconstruction in manufactured inhomogeneous steel-based materials

Mahendra Munidasa,[a] Frank Funak, and Andreas Mandelis[b]
Department of Mechanical Engineering, University of Toronto and Manufacturing Research Corporation of Ontario, 5 King's College Road, Toronto, Ontario, M5S 3G8 Canada

(Received 29 August 1997; accepted for publication 20 November 1997)

Several applications will be presented using an inversion methodology based on the generalized theoretical formulation [J. Appl. Phys. **80,** 5570 (1996)] of the Hamilton-Jacobi formulation of thermal-wave physics to the problem of photothermal radiometric depth profilometry of the thermal diffusivity of inhomogeneous solids. In the depth profile reconstruction algorithm three channels of information, namely, the amplitude, the phase, and the derivative of phase, of the photothermal signal are utilized to reduce multiple solutions to a single consistent and continuous solution. Wherever possible, diffusivity profiles are compared with those resulting from destructive microhardness testing. © *1998 American Institute of Physics.* [S0021-8979(98)04305-9]

I. INTRODUCTION

Thermal diffusivity which depends on the microstructural properties of a material, is very sensitive to the changes that take place in the material as a result of surface modification processes such as laser processing, case hardening and coating deposition. Considering this change in thermal diffusivity and the typical penetration depths involved (a few micrometers to a couple of millimeters), photothermal techniques have proven to be a good nondestructive and noncontact method of profiling these subsurface inhomogeneities.[1–3] Here the penetration depth is governed by the frequency-dependent thermal diffusion length $\mu=(2\alpha/\omega)^{1/2}$, where α is the thermal diffusion length and ω is the angular modulation frequency of the laser beam intensity.

In recent years several attempts have been made in inverting these data to reconstruct thermal diffusivity (conductivity) depth profiles, which are summarized in Ref. 4. In this article we will use the inversion methodology based on the generalized theoretical formulation described in Ref. 4 with added improvements, to investigate manufactured steel-based materials.

II. EXPERIMENTAL METHOD

A schematic diagram of the experimental apparatus is shown in Fig. 1. An Ar^+ laser (514 nm) modulated by an acousto-optic modulator is directed onto the sample surface. The emitted infrared (IR) radiation from the sample surface is collected and focused onto the detector using two off-axis paraboloidal mirrors.[5] The detector is a liquid N_2 cooled HgCdTe element with an active area of 1 mm^2 and a spectrally selective range of 2–12 μm. A germanium window with a transmission bandwidth of 2–14 μm is mounted in front of the detector to block any visible radiation from the pump laser. The pump beam spot size is made much larger than the maximum profiling depth, $\mu(\omega_{\min})$, to maintain the one-dimensional heat diffusion formalism assumed in the theory. The detector signal is preamplified before being sent to a lock-in amplifier. The lock-in amplifier outputs, amplitude and phase, are recorded at a range of laser modulation frequencies. A detailed description of this experimental procedure can be found elsewhere.[2]

III. THEORY

An exponential thermal diffusivity (α_s) profile of the form

$$\alpha_s(x)=\alpha_0\left(\frac{1+\Delta e^{-qx}}{1+\Delta}\right)^2 \tag{1}$$

is assumed, where

$$\Delta=\frac{1-\sqrt{\alpha_L/\alpha_0}}{\sqrt{\alpha_L/\alpha_0}-e^{-qL}} \tag{2}$$

and α_0, α_L, q are constants representing the values of the thermal diffusivity at the two boundary surfaces ($x=0$, L) of the inhomogeneous material layer, and the diffusivity gradient, respectively. The expression for the surface temperature $T(0,\omega)$ is given by[4]

$$\begin{aligned}T(0,\omega)=\Theta_0(\omega)(R_L-1)(e^{-\sigma_L J_L}-1)(1+de^{-H(L)}\\ -e^{-2H(L)})\left[1-\frac{R_L}{R_b}\left(\frac{1+\gamma_{bL}}{1-\gamma_{bL}e^{-2\sigma_L L}}\right)e^{-\sigma_L L}\right]\\ +\Theta_0(\omega)R_L\left(\frac{1+\gamma_{bL}e^{-2\sigma_L L}}{1-\gamma_{bL}e^{-2\sigma_L L}}\right),\end{aligned} \tag{3}$$

where Θ_0 is the thermal-wave field at the surface of a solid with constant thermophysical properties α_0 and k_0 and

[a]Current address: Valmet Automation (Canada) Ltd., 111 Granton Dr., Richmond Hill, ON L4B 1L5, Canada.
[b]Electronic mail: mandelis@me.utoronto.ca

$$\sigma_j=(1+i)\sqrt{\frac{\omega}{2\alpha_j}};\quad j\equiv 0,\ L, \tag{4a}$$

$$\gamma_{ij}\equiv\frac{1-R_{ij}}{1+R_{ij}};\quad R_{ij}\equiv\frac{e_i}{e_j};\quad R_j\equiv R_{0j}=\frac{R_0}{R_j}, \tag{4b}$$

$$H(L)=(1+i)\sqrt{\frac{\omega}{2\alpha_L}}\left[\frac{1-e^{-qL}}{1-\sqrt{(\alpha_0/\alpha_L)}e^{-qL}}\right]\left[L-\frac{1}{2q}\ln\left(\frac{\alpha_o}{\alpha_L}\right)\right]. \tag{4c}$$

Here $e_i=(k_i\rho_i c_i)^{1/2}$ is the thermal effusivity of material (i), with density ρ_i, specific heat c_i, and thermal conductivity k_i. Therefore, R_{ij} represents the thermal coupling coefficient at the interface between layers (i) and (j).

Furthermore,

$$\sigma_L J_L=\sigma_L L-H(L), \tag{4d}$$

$$de^{-H(L)}=\left[\left(\frac{1+\gamma_{b0}e^{-2\sigma_0 L}}{1-\gamma_{bo}e^{-2\sigma_0 L}}\right)-R_L\left(\frac{1+\gamma_{bL}e^{-2\sigma_L L}}{1-\gamma_{bL}e^{-2\sigma_L L}}\right)\right]\times\frac{e^{-[H(L)-\sigma_0 L]}}{(R_L-1)(e^{-(\sigma_L-\sigma_0)L}-1)[1-(R_L/R_b)\{(1+\gamma_{bL})/(1-\gamma_{bL}e^{-2\sigma_L L})\}e^{-\sigma_L L}]}+e^{-[\sigma_0 L+H(L)]}-e^{-[H(L)-\sigma_0 L]}. \tag{4e}$$

The surface temperature response to the incident optical beam on the sample is normalized by the surface temperature response to the same beam at the same frequency of a semi-infinite homogeneous material (reference). This gives a data pair for each frequency, namely amplitude ratio and phase difference between sample and reference. The normalizing procedure is necessary for the correct accounting of all frequency dependencies in the apparatus other than that due to the investigated sample. Theoretical values of the data pairs are calculated by Eq. (4) where

$$|M(\omega)|\times e^{i\Delta\phi(\omega)}=\text{Right-hand side of Eq. (3)}. \tag{5}$$

$|M(\omega)|$ is the amplitude ratio and $\Delta\phi(\omega)$ is the phase difference at angular frequency ω.

The values of amplitude, phase, and the derivative of the phase are compared with the experimental values in calculating the local parameters α_0, α_L, and q at each frequency using the numerical search algorithm described in Ref. 4. The method used is a multidimensional secant method known as Broyden's method.[6] Although in Ref. 4 only amplitude and phase were used, the general procedure is the same except for the fact that the addition of the use of the derivative of the phase allows for the search for all three parameters α_0, α_L, and q. Matching the derivative of the phase data to the derivative of the phase of the solution adds another constraint. This new approach considerably reduced the number of multiple solutions obtained prior to this development. The derivative of the phase data is calculated numerically and is used as an additional column of data along with amplitude and phase. The derivative is obtained with respect to 1/(frequency)$^{1/2}$ instead of frequency due to numerical reasons. In our earlier method[4] it was necessary to fix one parameter, and search for the other two. If the algorithm could not find a solution, the fixed parameter was changed manually and the search resumed. This was time consuming and also led to multiple solutions. Multiple solutions are an inevitable consequence of the ill-posed nature of the thermal-wave (and generally any diffusion-wave) inverse problem. The accepted solution is the one that has the maximum success rate in determining individual solutions at the experimental frequencies over the entire frequency range used. Inclusion of the derivative also allows the smooth transition of the solutions from one frequency to the next.

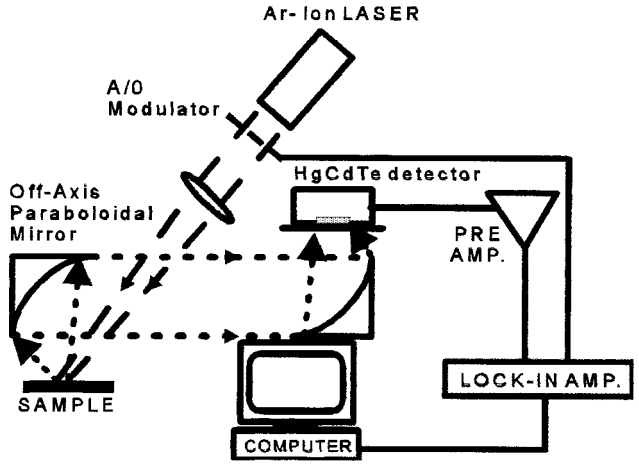

FIG. 1. Schematic diagram of the photothermal radiometric experimental setup.

In reconstructing depth profiles from data it is very important to first find a reliable set of initial values for α_0, α_L, and q. This could be achieved by finding the best fit to the first two to three points (high frequency end) to the theoretical values calculated from Eq. (4) assuming a single profile of the form given by Eq. (2).

IV. DATA AND RESULTS

We investigated two case-hardened steel samples made of C15 steel.[7] The surface hardening of these samples has

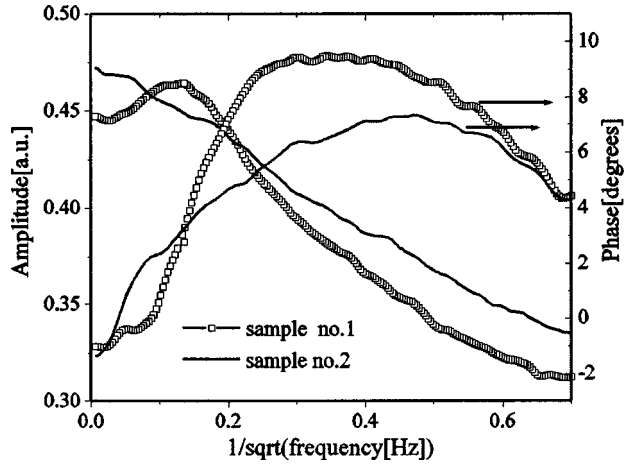

FIG. 2. Photothermal amplitude and phase data from two case-hardened steel samples of thickness 2 mm.

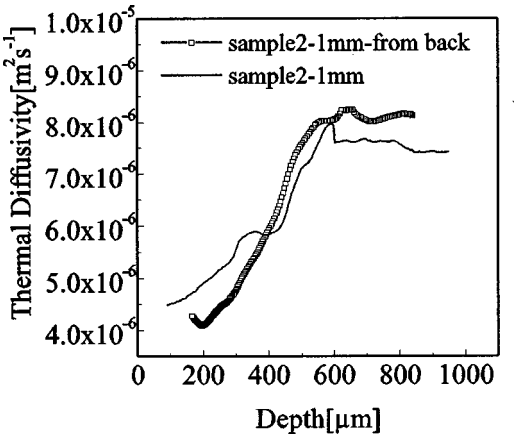

FIG. 4. Reconstructed profiles from the two sides of the 1 mm sample.

been achieved by dissolving additional carbon through the surface (carburization) and subsequent thermal treatment.[3] In the two samples investigated here, the thickness of the hardened layer was varied by changing the carburization time from sample to sample. The sample surfaces were polished to avoid any influence from surface roughness.

The photothermal amplitude and the phase data in the frequency range of 2 Hz–50 kHz obtained from the two samples normalized to a reference sample are shown in Fig. 2. The corresponding hardness profiles are shown in Fig. 3. The hardening depth for sample 1 is about 450 μm and for sample No. 2 it is 600 μm. The steel samples could be treated as layers of thickness L (in this case 2 mm) on a homogeneous substrate (air). The peak in the phase data and the sharp drop in the phase at low frequencies are clearly the results of the presence of the back boundary. A simple calculation using the average diffusivity of carbon steel and the Opsal and Rosencwaig theory[8] for a homogeneous layer of thickness L shows that the presence of the back boundary is ''seen'' (deviation from $-45°$ phase) in the backscattered signal from the front surface around 20 Hz which corresponds to a penetration depth of about 425 μm. Therefore, it is necessary to use a finite thickness layer theory for depth reconstruction in order to obtain a reliable profile beyond this depth for these samples. The resulting diffusivity profiles together with the available[7] microhardness profiles are shown in Fig. 3.

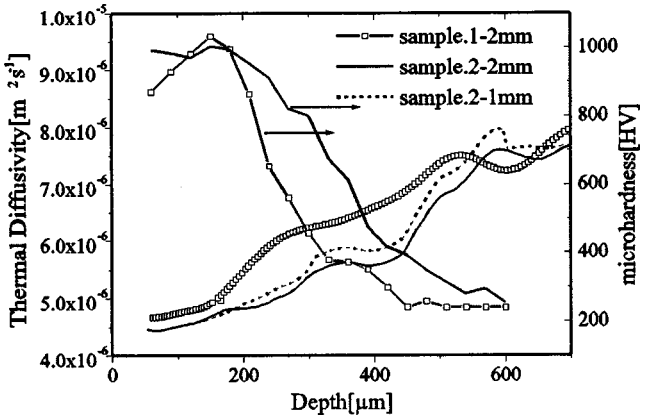

FIG. 3. Reconstructed thermal diffusivity depth profile from the data in Fig. 2 and the profile after machining sample No. 2 to 1 mm thickness for the case-hardened steel samples and the corresponding microhardness profiles.

Although our diffusivity profiles do not show an identical inverse relation to the hardness profiles, the variations from sample to sample are well correlated. It should be noted here that the microhardness measurements were performed[7] not on the same sample but on a different set of samples, assumed to be identical. The limiting factor that prohibited the profile to be obtained down to the other side of the samples from data taken from the opposite side was the three-dimensional (lateral) heat flow that was not taken into account in the theory. This effect becomes significant at depths $\geqslant$ 1 mm in the present samples.

To confirm the validity of our finite thickness reconstruction methodology the following procedure was performed. The sample No. 2 was machined down to a thickness of 1 mm from the side opposite to the profile shown in Fig. 3. Then data were collected again from the case-hardened side and also from the machined side. The reconstructed profiles are shown in Fig. 4. A portion of the profile obtained from the data taken from the hardened side of the 1-mm-thick sample No. 2 is also shown in Fig. 3 to compare with the profile reconstructed when that sample was 2 mm thick. The difference between those two profiles in Fig. 3 is the tolerance of our reconstruction methodology. The difference in the two profiles reconstructed from opposite sides can be attributed to the inability to obtain very reliable reconstructions at very low frequencies. The major reason for that is the three-dimensional effects which were not taken into account in the theory. Our experiments show that to keep the heat flow as one dimensional as possible, not only does the laser beam spot size have to be large compared to the thermal-wave penetration depth, but also the spatial intensity profile of the beam has to be flat. Even though the beam is very large, its Gaussian nature introduces three-dimensional effects which are difficult to normalize out. In future work it is recommended to insert Gaussian-beam flattening optics (''top-hat'' spatial distribution) to the beam delivery path of the radiometric system. Preliminary experiments performed with a finite-thickness homogeneous

sample and a gradually expanded Gaussian beam profile have shown that at low frequencies the signal phase decreases with increasing beam size but never reaches the one-dimensional theoretically expected value of $-45°$. Possible effects of machining of the steel samples on the thermal diffusivity depth profile are discussed in Ref. 4 and were found to be very small compared to the steep profiles seen in Fig. 4. It was thus concluded that the reconstructed profiles were hardly affected by the machining of the sample.

V. CONCLUSIONS

In this article we have described an improved, reliable nondestructive thermal-wave remote sensing method which allows the reconstruction of thermal diffusivity profiles in an inhomogeneous sample. The sample may be an inhomogeneous layer of finite thickness on a homogeneous substrate; a free standing layer, i.e., with air as the substrate; or a semi-infinite solid with its inhomogeneity continuously varying and attaining the value of the homogeneous bulk diffusivity. We have investigated case-hardened steel samples which show the potential of this technique as a nondestructive, non-contact quality control methodology for near-surface processing of materials. The quantitative diffusivity depth profiles obtained for case-hardened steel were found to anticorrelate, at least qualitatively, with destructive microhardness measurements.

ACKNOWLEDGMENTS

The support of the Manufacturing Research Corporation of Ontario is gratefully acknowledged. The authors would like to thank Professor H. G. Walther and his co-workers at Friedrich-Schiller-Universitat Jena, Jena, Germany for providing the case-hardened steel samples and the microhardness data of those samples.

[1] T.-C. Ma, M. Munidasa, and A. Mandelis, J. Appl. Phys. **71**, 6029 (1992).
[2] M. Munidasa, T. C. Ma, A. Mandelis, S. K. Brown, and L. Mannik, Mater. Sci. Eng. A **159**, 111 (1992).
[3] T. T. N. Lan, U. Seidel, H. G. Walther, G. Goch, and B. Schmitz, J. Appl. Phys. **78**, 4108 (1995).
[4] A. Mandelis, F. Funak, and M. Munidasa, J. Appl. Phys. **80**, 5570 (1996).
[5] T. M. Hiller, M. G. Somekh, S. J. Sheard, and D. R. Newcombe, Mater. Sci. Eng. B **5**, 107 (1990).
[6] W. H. Press, S. A. Teukolsky, W. T. Vetterling, and B. P. Flannery, *Numerical Recipes in C*, 2nd ed. (Cambridge University Press, Cambridge, 1992), p. 389.
[7] Courtesy: H. G. Walther's group, Friedrich-Schiller-Universitat Jena, Jena, Germany.
[8] J. Opsal and A. Rosencwaig, J. Appl. Phys. **53**, 4240 (1982).